

AN EXAMINATION OF THE SUNSPOT AREAL DATASET, 1875–2017: PAPER II, HEMISPHERIC DIFFERENCES

Robert M. Wilson
NASA Marshall Space Flight Center, NSSTC, Huntsville, Alabama

robert.m.wilson@nasa.gov

ABSTRACT

This is the second paper in an anticipated three-part study of the sunspot areal dataset. Examined are the annual variations of the northern (N) and southern (S) hemispheric sunspot area (SSA), number of active region entries (NARE), and the mean area per entry (MAE) for the interval 1875–2017, spanning solar cycles (SCs) SC12–SC24. For the overall interval of 1875–2019, SSA(N) has been larger than SSA(S) for 77 of the 145 years. Likewise, for SC12–SC24, SSA(N) has been greater than SSA(S) during the ascending phase of the solar cycle (i.e., 35 of 52 years), whether the SC is an even- or odd-numbered SC, while SSA(S) has been greater than SSA(N) during the descending phase of the solar cycle (51 of 93 years). Minimum SSA(N) and SSA(S) have occurred in the same year in only 7 of 13 SCs, including SC14, SC16 and SC19–SC23. Maximum SSA(N) and SSA(S) have occurred in the same year only once (in SC15). Maximum SSA(S) usually occurs after maximum SSA(N), true for 9 of 13 SCs. Maximum SSA(S) preceded maximum SSA(N) in SC16, SC18, and SC19. Multiple peaks in SSA(N) or SSA(S), typically 2–3 years apart, have often been seen (e.g., SC12–SC16 and SC18–SC22). SC12 had the smallest maximum SSA(N) (452.0 millionths of a solar hemisphere), while SC19 had the largest maximum SSA(N) (2,277.2 millionths of a solar hemisphere). SC14 had the smallest SSA(S) (600.3 millionths of a solar hemisphere), while SC18 had the largest SSA(S) (1,642.9 millionths of a solar hemisphere). The average time from minimum to maximum SSA(N) is 3.8 years (range 2–5 years), while it is 4.8 years for SSA(S) (range 3–6 years). The average time from maximum SSA(N) to the following minimum SSA(N) is 6.9 years (range 5–9 years), while it is 6.2 years for SSA(S) (range 5–8 years). The largest N-S asymmetry coefficients for SSA occurs between –3 and +1 years about sunspot minimum. The largest N-S asymmetry coefficient in SSA occurred in 2019 (SC24). The largest area sunspot occurred in 1947 (SC18) in the southern hemisphere and measured 6,132 millionths of a solar hemisphere, nearly twice the size of the average maxima of the largest area spots in the other 12 SCs. SSA and NARE are highly correlated with each other and with SSN. Minimum MAE(N) and MAE(S) may have occurred, respectively, in 2018 and 2019, highly suggestive that SSN(m) for SC25 either occurred in 2019 or will occur in 2020.

INTRODUCTION

This is the second paper in an anticipated three-part study of the sunspot areal dataset, 1875–2017. Paper I (Wilson 2020) provided a general overview of the sunspot areal dataset, examining—in particular—the annual variations of selected parameters and inferred correlations that are apparent in the sunspot areal dataset. This paper (Paper II) examines the hemispheric

differences of selected parameters using the sunspot areal database. Paper III will examine annual variations of the magnetic complexity of sunspots.

North-South (N-S) asymmetry has long-been recognized by solar observers as related to the distributions of major flare events, sunspot magnetic classes and sunspot areas. For example, Newton and Milson (1955) studied the N-S asymmetry of sunspot areas during the interval 1874–1954 and concluded that the fluctuations are real, their work following previous work reported by Newcomb (1901), Maunder (1922) and Kiepenheuer (1953). Later, Waldmeier (1971) investigated the N-S asymmetry of sunspots during the interval 1874–1969, arguing that the real asymmetry was strengthened by a phase difference of the two hemispheres, where the phase shift is subject to a long period that contains eight 11-year SCs. Roy (1977) noted that magnetically complex sunspot groups displayed a more pronounced asymmetry during the interval 1962–1970 than noncomplex groups. Antalová and Gnevyshev (1983) found that an N-S sunspot area asymmetry was a persistent feature, especially for SC14–SC20. Swinson et al. (1986) noted that, in general, northern hemispheric activity peaked about 2 years after sunspot minimum, with even-numbered cycles having a greater peak in northern hemispheric activity. Vizoso and Ballester (1987) examined the N-S asymmetry in sudden disappearances of solar prominences, noting that it does not appear to be in phase with the solar cycle, instead peaking about the time of solar minimum and reversing in sign during solar maximum. Garcia (1990) noted that the N-S distribution of large flares appears periodic and approximately in phase with the solar cycle, with the most intense large flares showing the largest N-S asymmetry. Vizoso and Ballester (1990) performed an exhaustive study of the N-S asymmetry of sunspots during the interval 1874–1976 and found: (1) that the N-S asymmetry is statistically significant, (2) the highest values of the N-S asymmetry coefficient for sunspots are obtained around sunspot minimum, and (3) there is a long-term periodic behavior of about eight cycles in which the activity in one hemisphere is more important during the ascending branch while during the descending branch the activity becomes more important in the opposite hemisphere. Through the years, many other studies have followed, investigating the N-S asymmetry of sunspots/solar flares including, in part: Schlamminger (1991); Yi (1992); Carbonell et al. (1993); Oliver and Ballester (1994); Duchlev and Dermendjiev (1996); Watari (1996); Ataç and Özgüç (1996); Vernova et al. (2002); Temmer et al. (2002, 2006); Li, Wang, Xiong, et al., (2002); Li, Chen, Zhan, Shi et al. (2009); Li, Gao, Zhan (2008); Li, Gao, Zhan et al. (2009); Knaack et al. (2004); Joshi and Joshi (2004); Vernova et al. (2004); Ballester et al. (2005); Zharkov et al. (2005); Zolotova and Ponyavin (2006); Zolotova and Ponyavin (2007); Chang (2007, 2008); Li (2009); Donner and Thiel (2007); Zolotova et al. (2009); Badalyan and Obridko (2011); and Chowdhury et al. (2013).

In this Paper (II), several issues regarding the asymmetry of sunspots are examined, including: (1) the variation of the N and S hemispheric annual SSAs for the interval 1875–2017 in relation to SSN minimum (m) and maximum (M) occurrences, (2) the variation of the N- and S-hemispheric annual NARE, (3) the variation of N- and S-hemispheric annual MAE, (4) the annual asymmetry coefficients for SSA and NARE, and (5) the results of epoch analyses for these parameters based on SSN(m) occurrence.

METHODS AND MATERIALS

Two primary data sources are used in this study: (1) annual values of SSN, available online at <http://sidc.oma.be/silo/datafiles> and (2) annual values of SSA, available online at <http://solarcyclescience.com/activeregions.html>. Other parameters taken from the SSA dataset

(Greenwich Observatory (RGO) interval 1875–1976) and the United States Air Force/National Oceanic and Atmospheric Administration (USAF/NOAA) interval 1977–2019) include (1) NARE and (2) MAE, where MAE is computed as SSA divided by NARE times the number of days in the year.

RESULTS AND DISCUSSION

Table 1 provides the basic data used in this investigation, spanning the interval 1875–2017. The yearly 2018 and 2019 values are also shown but have not been included in the parametric means, which are given at the bottom of the table, both in terms of overall means (and standard deviations, *sd*) and even- and odd-numbered sunspot cycle means (and *sd*). Given in table 1 are the (1) NARE, (2) SSA, (3) MAE, and (4) asymmetry for NARE and SSA. For NARE, SSA, and MAE, the yearly N hemispheric, S hemispheric, and combined (C) hemispheric parametric values are given. Also given is each cycle’s largest observed area (active region), denoted LAAR, and the hemisphere (H) in which it occurred. Also identified are the m and M parametric values for each SC, SC12–SC24.

Table 1. N-S hemispheric values of NARE, SSA and MAE, along with SSN, LAAR/H and asymmetry of NARE and SSA, 1875–2017.

Year	SSN	NARE			SSA		MAE			LAAR/H	Asymmetry		
		C	N	S	C	N	S	C	N		S	NARE	SSA
1875	28.3	394	222	172	213.1	123.0	90.2	197	202	191	981/N	0.127	0.154
1876	18.9	265	83	182	109.3	34.6	74.7	151	153	150	711/S	-0.374	-0.367
1877	20.7	229	106	123	92.9	35.4	57.4	148	122	170	778/S	-0.074	-0.237
SC12													
1878	5.7m	81m	66	15m	22.2m	20.5	1.7m	100m	113	41m	402/N,m	0.630M	0.847M
1879	10.0	117	53m	64	36.3	11.9m	24.4	113	82m	139	464/S	-0.094M	-0.344
1880	53.7	775	467	308	446.8	271.4	175.3	211	213M	208	1,449/N	0.205	0.215
1881	90.5	1,423	894	529	679.5	452.0M	227.5	174	185	157	1,227/N	0.257	0.330
1882	99.0	1,622	895M	727	968.0	441.9	526.1	218	180	264	2,425/N,M	0.104	-0.087m
1883	106.1M	1,792	661	1,131	1,148.9M	328.0	820.9M	234M	181	265M	1,876/N	-0.262	-0.429
1884	105.8	2,039M	833	1,206M	1,034.1	451.3	582.8	186	198	177	2,246/S	0.183	-0.127
1885	86.3	1,522	505	1017	810.2	282.9	527.3	194	204	189	1,917/M	-0.336	-0.302
1886	42.4	750	239	511	379.4	97.4	282.0	185	149	201	1,125/M	-0.363	-0.487
1887	21.8	452	145	307	177.3	43.4	133.9	143	109	159	1,030/S	-0.358	-0.510
1888	11.2	265	50	215	87.9	19.5	68.5	121m	143	116m	786/S	-0.623	-0.557
SC13													
1889	10.4m	191m	29m	162	76.7m	4.7m	72.0	147	59m	162	639/S,m	-0.696M	-0.877M
1890	11.8	258	116	142m	98.9	53.4	45.4m	140	168	117	1,135/S	-0.101	0.081
1891	59.5	1,252	881	371	566.4	399.1	167.4	165	165	165	1,798/N	0.407	0.409
1892	121.7	2,321	1,193	1,128	1,211.3	602.0M	609.2	191	185	198	3,038/S,M	0.028	-0.006m
1893	142.0M	3,072M	1,264M	1,808M	1,460.6M	516.6	944.0M	174	149	191	2,621/S	-0.177	-0.293
1894	130.0	2,740	1,258	1,482	1,281.5	544.6	736.9	171	158	181	2,511/S	-0.082	-0.150
1895	106.6	2,134	1,076	1,058	973.4	567.5	406.0	166	193	140	1,722/S	0.008m	0.285
1896	69.4	1,182	379	803	547.4	206.0	341.5	169	199M	157	2,458/N	-0.359	-0.248
1897	43.8	903	393	510	511.7	182.8	328.9	207M	170	235M	2,743/S	-0.130	-0.286
1898	44.4	777	271	506	374.7	108.5	266.2	176	146	192	2,235/S	-0.302	-0.421
1899	20.2	385	86	299	110.0	23.4	86.6	104	99	106	638/S,m	-0.553M	-0.575M
1900	15.7	273	120	153	74.3	26.8	47.5	100m	82m	114	750/S	-0.121	-0.279
SC14													
1901	4.6m	78m	36m	42m	27.9m	21.2m	6.6m	131	215	57m	699/N	-0.077m	0.523
1902	8.5	134	87	47	59.5	39.9	19.6	162	167	152	1,113/N	0.299	0.341
1903	40.8	760	330	430	338.6	131.5	207.1	163	145	176	2,129/S	-0.132	-0.223
1904	70.1	1,374	825	549	488.2	268.5	219.7	130	119	146	1,532/N	0.201	0.100
1905	105.5M	1,937	1,145	792	1,195.9M	749.3M	446.6	225M	239M	206	3,339/S,M	0.182	0.253
1906	90.1	1,859	1,235M	624	775.0	535.5	239.5	152	158	140	1,470/S	0.329	0.382
1907	102.8	1,951M	898	1,053M	1,092.1	491.8	600.3M	204	200	208M	2,555/S	-0.079	-0.099
1908	80.9	1,687	698	989	697.5	316.5	381.0	151	166	141	1,919/N	-0.172	-0.092m
1909	73.2	1,442	577	865	691.5	297.0	394.5	175	188	166	1,959/S	-0.200	-0.141

Year	NARE			SSA			MAE			Asymmetry			
	SSN	C	N	S	C	N	S	C	N	S	LAAR/H	NARE	SSA
1910	30.9	766	207	559	266.0	64.8	201.3	127	114	131	1,139/S	-0.460	-0.513
1911	9.5	279	78	201	64.4	21.6	42.8	84	101	78	332/N	-0.441	-0.329
1912	6.0	154	11m	143	37.3	0.8m	36.6	89	127m	94	685/S	-0.857M	-0.960M
SC15													
1913	2.4m	60m	39	21m	7.5m	5.1	2.5m	46m	48	43m	138/N,m	0.300	0.347
1914	16.1	436	225	211	152.4	99.1	53.3	128	161	92	817/N	0.032	0.301
1915	79.0	1,864	1,012	852	697.8	380.2	317.6	137	137	136	1,901/S	0.086	0.090m
1916	95.0	2,290	1,414	876	725.5	470.0	255.4	116	122	107	1,775/N	0.235	0.296
1917	173.6M	3,510M	1,938M	1,572M	1,533.9M	853.6M	680.4M	160	161	158	3,590/S,M	0.104	0.113
1918	134.6	2,904	1,500	1404	1,112.6	608.3	504.3	140	148	131	1,749/S	0.033	0.093
1919	105.7	2,249	991	1258	1,054.7	565.4	489.3	171M	208M	142	1,776N	-0.119	0.072
1920	62.7	1,396	678	718	617.3	207.8	409.5	162	112	209M	2,690/S	-0.029m	-0.327
1921	43.5	943	516	427	419.6	250.2	169.4	162	177	145	1,709/S	0.094	0.193
1922	23.7	543	314	229	252.0	160.0	92.0	169	186	147	1,478/N	0.157	0.270
SC16													
1923	9.7m	244m	138m	106m	54.7m	32.6m	22.0m	82m	86m	76m	831/N,m	0.131	0.194
1924	27.9	589	452	137	278.0	233.7	44.4	173	189	119	1,387/N	0.535M	0.681M
1925	74.0	1,718	1,072	646	825.1	513.7	311.3	175	175	176	2,934/N	0.248	0.245
1926	106.5	2,210	1,107	1,103	1,263.2	661.3	601.8	209M	218M	199M	3,716/N,M	0.002m	0.047m
1927	114.7	2,369	941	1,428M	1,060.8	379.0	681.9M	163	147	174	1,562/N	-0.206	-0.286
1928	129.7M	2,613M	1,301M	1,312	1,388.9M	725.9M	663.0	195	204	185	2,587/S	-0.004	0.045
1929	108.2	2,413	1,256	1,157	1,238.9	650.6	588.3	187	189	186	2,003/N	0.041	0.050
1930	59.4	1,394	798	596	516.6	286.1	230.6	135	131	141	1,506/N	0.145	0.107
1931	35.1	781	514	267	279.1	204.2	74.9	130	145	102	1,882/N	0.316	0.633
1932	18.6	471	283	188	163.2	122.7	40.5	127m	159	79	1,155/N,m	0.202	0.504
SC17													
1933	9.2m	225m	200	25m	91.3	89.5	1.8m	148	163	26m	1,594/N	0.778M	0.961M
1934	14.6	337	156m	181	118.2	44.3m	73.9	128	104m	149	1,169/S	-0.074	-0.250
1935	60.2	1,290	558	732	622.1	203.3	418.8	176	133	209	2,435/S	-0.135	-0.346
1936	132.8	2,706	1,214	1,492	1,140.8	462.6	678.2	154	139	166	1,641/S	-0.103	-0.189
1937	190.6M	3,705M	2,114M	1,591	2,072.8M	1,316.1M	756.7	204	227	174	3,340/N	0.141	0.270
1938	182.6	3,401	1,690	1,711M	2,015.2	886.0	1,129.2M	216	191	241M	3,627/N,M	-0.006m	-0.121
1939	148.0	2,892	1,330	1,562	1,576.8	645.1	931.7	199	177	218	3,054/S	-0.080	-0.182
1940	113.0	2,118	938	1,180	1,037.2	497.0	540.1	179	194	168	2,860/N	-0.114	-0.042m
1941	79.2	1,473	848	625	658.1	434.4	223.7	163	187	131	3,088/N	0.151	0.320
1942	50.8	1,014	527	487	427.3	256.2	171.2	154	177	128	2,048/N	0.039	0.199
1943	27.1	495	343	152M	296.8	250.9	45.9m	219M	267M	110m	1,892/N	0.386M	0.691M
SC18													
1944	16.1m	370m	135m	235	124.7m	42.2m	82.5	123m	114m	128	1,010/S,m	-0.270	-0.323
1945	55.3	1,103	369	734	426.5	119.4	307.2	141	118	153	1,142/S	-0.331	-0.440
1946	154.3	2,838	1,389	1,449	1,823.9	1,116.2	707.7	235M	293M	178	5,202/N	-0.021m	0.224
1947	214.7M	4,298M	1,930	2,368M	2,634.1M	991.1	1,642.9M	224	187	253M	6,132/S,M	-0.102	-0.247
1948	193.0	3,892	1,809	2,083	1,974.6	934.1	1,040.5	186	189	183	2,434/S	-0.070	-0.054m
1949	190.7	3,903	2,177M	1,726	2,140.0	1,180.2M	959.8	200	198	203	2,471/N	0.116	0.103
1950	118.9	2,333	1,396	937	1,227.3	776.2	451.2	192	203	176	2,856/N	0.197	0.265
1951	98.3	1,861	1,044	817	1,135.3	729.9	405.4	223	255	181	4,865/N	0.122	0.286
1952	45.0	963	457	506	402.9	194.7	208.2	153	156	151	1,212/S	-0.051	-0.034
1953	20.1	431	265	166	145.1	105.9	39.2	123	146	86m	1,062/N	0.230	0.460M
SC19													
1954	6.6m	166m	93m	73m	34.6m	11.7m	22.9m	76m	46m	115	712/S,m	0.120	-0.324
1955	54.2	1,183	746	437	552.4	328.5	223.9	170	161	187	1,449/N	0.261M	0.189
1956	200.7	3,820	1,911	1,909	2,394.7	1,242.8	1,151.9	229	238	221	2,306/S	0.001m	0.038m
1957	269.3M	4,855	2,295	2,560M	3,048.5M	1,446.6	1,601.9	229	230	228	2,480/S	-0.055	-0.051
1958	261.7	5,016M	2,630	2,386	3,011.3	1,402.5	1,608.8M	219	195	246M	2,256/N	0.049	-0.069
1959	225.1	4,514	3,173M	1,341	2,872.9	2,277.2M	595.8	232M	262M	162	2,805/N,M	0.406	0.585
1960	159.0	3,259	2,001	1,258	1,641.2	1,051.7	589.5	184	192	172	2,301/N	0.228	0.282
1961	76.4	1,586	1,008	578	613.5	444.5	169.0	141	161	107	1,445/N	0.271	0.449
1962	53.4	1,027	709	318	463.5	324.3	139.2	165	167	160	1,841/N	0.381	0.399
1963	39.9	819	630	189	287.8	228.1	59.7	128	132	115	1,311/N	0.538	0.585
SC20													
1964	15.0m	390m	284m	106	53.9m	44.1m	9.8m	51m	57m	34m	545/S,m	0.456	0.636
1965	22.0	506	429	77m	113.3	97.2	16.1	82	83	76	736/N	0.696M	0.716
1966	66.8	1,498	1,266	232	592.6	535.4	57.2	144	154	90	1,600/N	0.690	0.807M
1967	132.9	3,390M	2,159M	1,231	1,519.1	1,033.6M	485.6	164	175	144	2,235/N	0.274	0.361
1968	150.0M	2,963	1,588	1,375	1,569.8	961.2	608.6	194M	222M	162	3,202/N,M	0.072	0.225
1969	149.4	2,932	1,678	1,254	1,450.1	922.5	527.6	181	201	154	2,274/N	0.145	0.272
1970	148.0	3,379	1,757	1,622M	1,601.3M	918.0	683.3M	173	191	154	2,511/N	0.040	0.147
1971	94.4	2,229	1,121	1,108	990.2	455.0	534.8	162	148	176M	2,330/S	0.006	-0.080

Year	SSN	NARE			SSA			MAE			LAAR/H	Asymmetry	
		C	N	S	C	N	S	C	N	S		NARE	SSA
1972	97.6	2,263	877	1,386	916.7	328.4	588.3	148	137	155	2,250/S	-0.225	-0.284
1973	54.1	1,203	596	607	457.6	227.4	230.2	139	139	138	919/N	-0.009m	-0.006m
1974	49.2	1,096	384	712	398.9	138.2	260.6	133	131m	134	2,706/S	-0.299M	-0.307
1975	22.5	473	290	183m	166.4m	122.0	44.5m	128m	154	89m	1,295/N	0.226	-0.466M
SC21													
1976@	18.4m	426m	198m	228	169.8	95.0m	74.8	146	176	120	937/S	-0.070	0.119
1977	39.3	926	580	346	347.0	211.3	135.7	137	133	143	1,170/N	0.253	0.218
1978	131.0	4,035	2,247	1,788	1,368.5	854.5	514.1	124	139	105	1,920/N	0.114	0.249
1979	220.1M	5,438M	2,904M	2,534M	2,194.5	1,289.9M	904.6	147	162	130	1,720/S	0.068	0.176
1980	218.9	3,965	1,936	2,029	2,160.7	933.6	1,227.1M	199	176	221	2,300/S	-0.023m	-0.136
1981	198.9	3,920	2,038	1,882	2,270.2M	1,078.3	1,192.0	211	193	231M	2,301/S	0.040	-0.050
1982	162.4	3,686	1,759	1,927	2,220.1	1,088.9	1,131.3	220M	226	214	3,100/N,M	-0.046	-0.019m
1983	91.0	2,371	699	1,672	919.5	224.8	694.7	142	117	152	2,110/S	-0.410M	-0.511M
1984	60.5	1,474	524	950	811.7	355.8	456.0	202	249M	176	2,590/S	-0.289	-0.123
1985	20.6	604	280	324	179.0	81.2	97.7	108m	106	110	840/N	-0.073	-0.092
SC22													
1986	14.8m	394m	242m	152m	123.2m	80.4m	42.8m	114	121	103m	700/S,m	0.228	0.305
1987	33.9	938	340	598	293.8	97.0	196.8	114	104m	120	800/N	-0.275	-0.340
1988	123.0	2,900	1,591	1,309	1,343.4	674.2	669.1	170	155	187	2,900/S	0.097	0.004
1989	211.1M	4,734	2,532M	2,202	2,572.0M	1,363.8M	1,208.3	198M	197m	200M	3,600/N,M	0.070	0.060
1990	191.8	4,751M	2,202	2,549	2,053.2	1,039.0	1,014.2	158	172	145	3,080/N	-0.073	0.012
1991	203.3	4,715	1,798	2,917M	2,499.2	943.0	1,555.8M	193	192	195	2,530/S	-0.237	-0.245
1992	133.0	3,314	1,287	2,027	1,380.8	553.0	827.9	152	157	149	1,650/S	-0.223	-0.199
1993	76.1	1,886	941	945	717.2	358.7	358.5	138	139	138	1,230/S	-0.002m	0.000m
1994	44.9	1,205	566	639	361.4	215.1	146.3	109	139	84m	940/N	-0.061	0.190
1995	25.1	707	293	414	169.0	61.3	107.7	87m	76	95	1,800/S	-0.171	-0.275
SC23													
1996	11.6m	305m	182m	124m	81.9m	26.9m	55.0m	98	54m	162	880/S,m	0.190	-0.343M
1997	28.9	686	432	254	208.6	111.5	97.1	111	94	140	1,000/S	0.259M	0.069
1998	88.3	1,937	914	1,023	760.8	335.5	425.3	143	134	152	1,460/S	-0.056	-0.118
1999	136.3	2,733	1,551	1,182	1,164.3	687.8	476.6	155	162	147	1,370/N	0.135	0.181
2000	173.9M	3,587M	1,822	1,765	1,609.7	829.7	780.0	164	167	162	2,140/N	0.016m	0.031
2001	170.4	3,476	1,863M	1,613	1,707.4	922.8M	784.6	179	181	178	2,440/N	0.072	0.081
2002	163.6	3,528	1,588	1,940M	1,833.8M	729.9	1,103.9M	190	168	208	1,990/S	-0.100	-0.204
2003	99.3	2,145	928	1,217	1,099.5	549.7	549.8	187	216	165	2,610/S,M	-0.135	-0.000m
2004	65.3	1,311	446	865	683.3	270.7	412.6	191	222M	175	2,010/N	-0.320	-0.208
2005	45.8	973	364	609	542.5	188.6	353.9	204M	189	212M	1,630/N	-0.252	-0.305
2006	24.7	600	114	486	245.0	19.8	225.2	149	63	169	750/S	-0.620	-0.838M
2007	12.6	308	58	250	134.4	12.3	122.1	159	77	178	540/S	-0.623M	-0.817
SC24													
2008	4.2m	122m	41m	81	22.9m	5.0m	17.8	69m	45m	80	300/S,m	-0.328	-0.559
2009	4.8	123	85	38m	26.1	18.1	7.9m	77	78	76m	380/N	0.382	0.391
2010	24.9	623	396	227	214.2	150.8	63.4	125	139	102	550/N	0.271	0.408
2011	80.8	1,788	1,194M	594	747.2	561.4M	185.8	153	172M	114	1,540/N	0.336	0.503
2012	84.5	1,848	965	883	798.6	405.9	392.8	158	154	163	1,460/S	0.044	0.016
2013	94.0	2,121	886	1,235	860.0	361.0	499.0	148	149	147	1,100/N	-0.165	-0.160
2014	113.3M	2,442M	894	1,548M	1,251.0M	310.2	940.8M	187M	127	222	2,750/S,M	-0.268	-0.504
2015	69.8	1,544	783	761	621.4	306.5	315.0	147	143	151	1,190/S	0.014m	-0.014m
2016	39.9	910	665	245	317.0	218.5	98.5	127	120	147	850/N	0.462	0.379
2017	21.7	477	343	134	217.5	133.5	84.0	166	142	229M	1,060/S	0.438	0.228
2018	7.0	161	94	67	24.4	12.7	11.7	55	49	64	240/S	0.168	0.041
2019	3.6	97	89	8	17.3	17.1	0.2	103	70	9	420/N	0.835M	0.977M
mean			873.3	852.7		425.0	412.5		157	154		0.009	0.020
sd			703.6	680.6		399.5	381.4		49	47		0.281	0.363
even cycles													
mean			803.2	795.7		386.6	383.9		153	148		0.019	0.045
sd			616.0	657.8		344.5	362.4		50	50		0.295	0.369
odd cycles													
mean			950.7	915.6		467.2	444.1		160	160		-0.004	-0.009
sd			786.6	704.4		451.4	401.6		50	44		0.265	0.345

Note: Asymmetry = (N-S)/C, where C is the combined total (=N+S)

@ means end of the RGO dataset.

The largest individual spot group was active region 1488603, having a corrected area spot size of 6,132 millionth of a solar hemisphere on 04/08/1947 and designated RGO type 8.

Table 2 provides a simple comparison of the timing occurrences of *m* and *M* for *N* and *S* parametric values with respect to the occurrences of SSN(*m*) and SSN(*M*), where the value ‘0’ denotes that the parametric values occurred simultaneously (same year) with the corresponding SSN(*m*) and SSN(*M*) occurrences. Positive numbers indicate that the parametric values occurred (in years) after the corresponding SSN(*m*) and SSN(*M*) occurrences, while negative numbers indicate that the parametric values occurred (in years) before the corresponding SSN(*m*) and SSN(*M*) occurrences. Also given are the ascent (ASC) and descent (DES) intervals (in years) for each SC, where ASC is the time from to SSN(*m*) to SSN(*M*) for cycle *n*, while DES is the time from SSN(*M*) for cycle *n* to SSN(*m*) for cycle *n* + 1.

Table 2. Comparison of parametric *m* and *M* hemispheric occurrences with respect to corresponding occurrences of SSN(*m*) and SSN(*M*).

SC	SSA(N)		SSA(S)		NARE(N)		NARE(S)		MAE(N)		MAE(S)			
	ASC	DES	SSA (m)	SSA (M)	NARE (m)	NARE (M)	NARE (m)	NARE (M)	MAE (m)	MAE (M)	MAE (m)	MAE (M)		
12	5	6	+1	-2	0	0	+1	-1	0	+1	+1	-3	0	0
13	4	8	0	-1	+1	0	0	0	+1	0	0	+3	-1	+4
14	4	8	0	0	0	+2	0	+1	0	+2	-1	0	0	+2
15	4	6	-1	0	0	0	-1	0	0	0	-1	+2	0	0
16	5	5	0	0	0	-1	0	0	0	-1	0	-2	0	-2
17	4	7	+1	0	0	+1	+1	0	0	+1	+1	+6	0	+1
18	3	7	0	+2	-1	0	0	+2	-1	0	0	-1	-1	0
19	3	7	0	+2	0	+1	0	+1	0	+2	0	+2	-1	+1
20	4	8	0	-1	0	2	0	-1	+1	-1	0	0	0	+3
21	3	7	-1	0	-1	+1	0	0	-1	0	-2	+3	-1	+2
22	3	7	0	0	0	+2	0	0	0	+2	+1	0	0	0
23	4	8	0	+1	0	+2	0	+1	0	+2	0	+4	-2	+2
24	6	≥4#	0	-3	+1	0	0	-3	+1	0	0	-3	+1	+3

Note: # means SC24 DES is unknown; assumes SC25 in 2019.

Figures 1–3 display the annual variations of (1) (a) SSA(N) and (b) SSA(S), (2) (a) NARE(N) and (b) NARE(S), and (3) (a) MAE(N) and (b) MAE(S), respectively. Across the top of figures 1 and 2 are identified the years when SSN(*m*) and SSN(*M*) occurred per SC (located along the bottom in fig. 3), where SSN(*m*) occurrences are shown as unfilled triangles and SSN(*M*) occurrences are shown as filled triangles. The data intervals are divided according to whether the values come from the RGO record (1875–1976) or the extended record based on the USAF/NOAA observations (1977–present). The horizontal line in each figure gives the overall mean (given to the right along with *sd*) for the interval 1875–2017 and the numbers SC12–SC24 refer to the specific SCs. Plainly, the years 2018/2019 represent transitional years between the ending of SC24 and the onset of SC25, which is anticipated to occur either in late 2019 or 2020,

based on smoothed monthly mean SSN (cf. Wilson 2019a, 2019b, 2020). (It is now known that SC25 minimums for SSN and SSA occurred in 2019.)

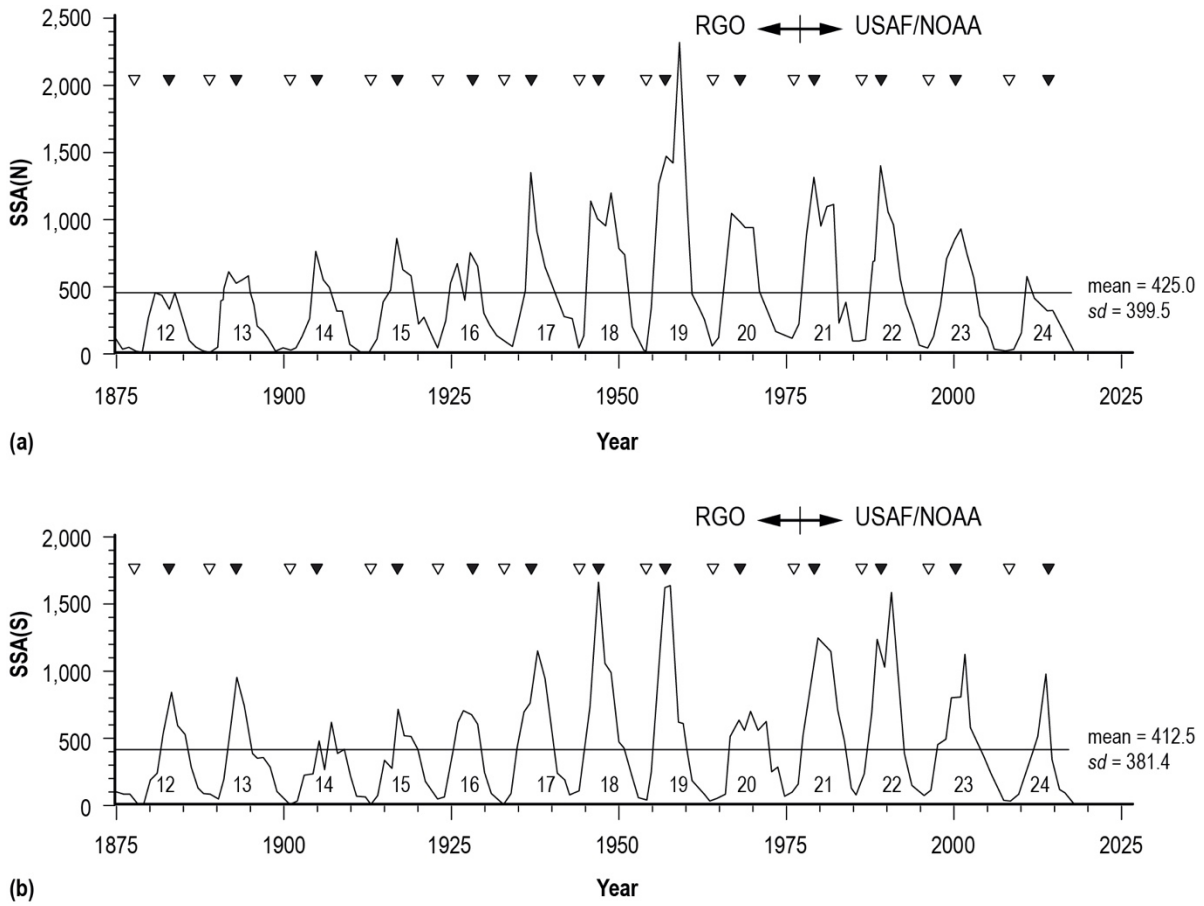


Figure 1. Annual variation of (a) SSA(N) and (b)SSA(S).

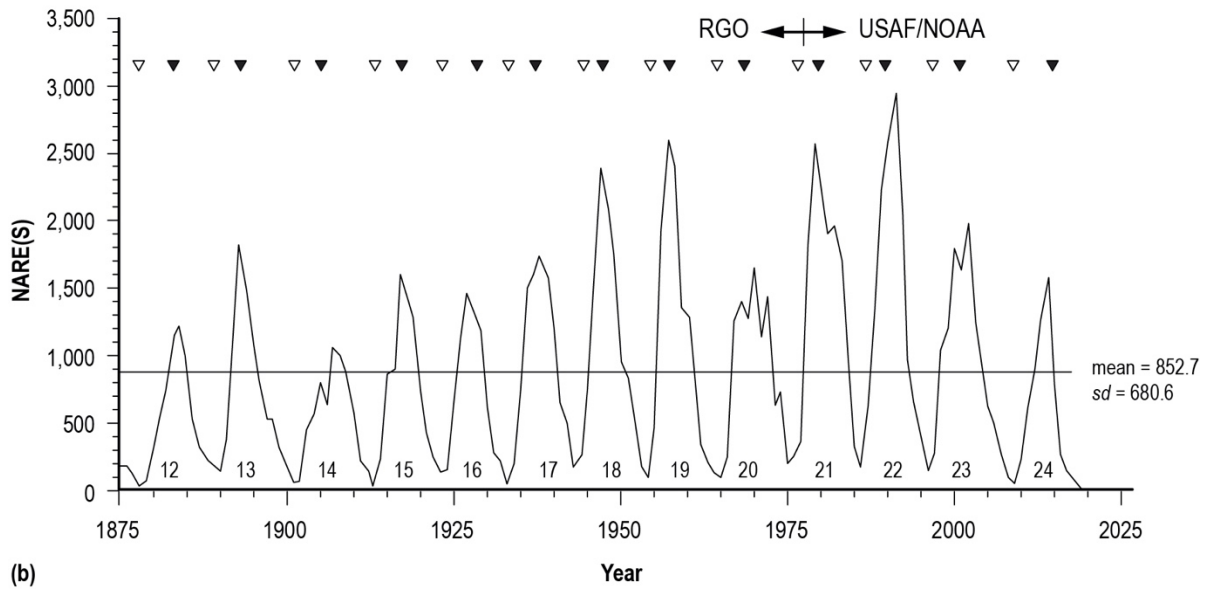
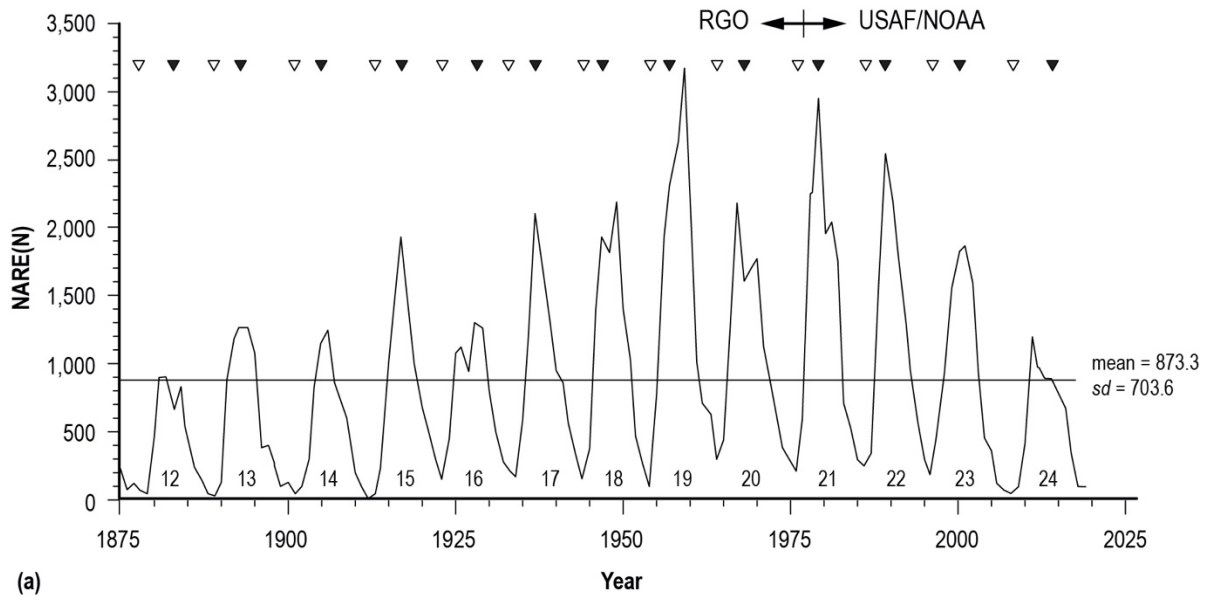


Figure 2. Annual variation of (a) NARE(N) and (b) NARE(S).

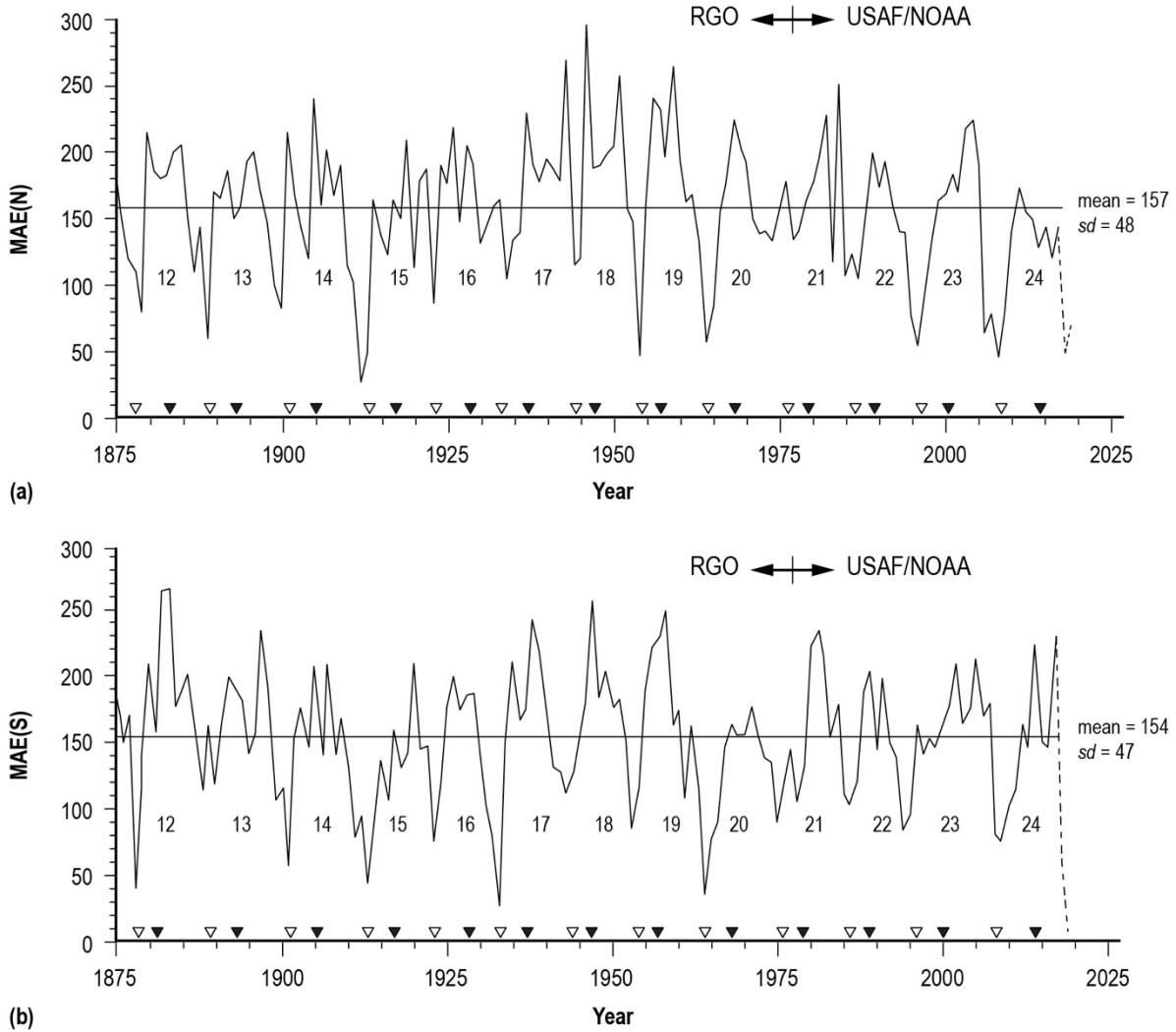


Figure 3. Annual variation of (a) MAE(N) and (b) MAE(S).

Figure 1a shows that the maximum in SSA(N) per SC increased between SC12 and SC19 and decreased between SC19 and SC24. SC19 had the largest yearly SSA(N), measuring 2,277.2 millionths of a solar hemisphere and occurring in 1959, some 2 years after SC19 SSN(M). The timing of the maximum for SSA(N) has occurred simultaneously with the maximum SSN(M) for only 6 of 13 SCs. For SC12, SC13, SC20, and SC24, maximum SSA(N) preceded SSN(M), while for SC18, SC19 and SC23, maximum SSA(N) followed SSN(M). Minimum SSA(N) nearly always has occurred simultaneously with SSN(m), with only SC12, 17, and 21, having minimum SSA(N) occurrences that differed by 1 year from SSN(m).

Figure 1b shows that the maximum in SSA(S) per SC also increased, especially, between SC14 and SC18–SC19 and decreased afterwards through SC24. The largest yearly SSA(S) measured 1,642.9 millionths of a solar hemisphere and occurred in 1947 (SC18), simultaneously with SC18 SSN(M). The timing of maximum in SSA(S) is found to have followed SSN(M) in 7 of 13 SCs, occurring simultaneously in 5 of 13 SCs and preceded by one year only in SC16. Like SSA (N), the minimum in SSA(S) usually occurs simultaneously with SSN(m), with only SC14,

SC16, SC17, and SC21 having minimum SSA(S) occurrences that differed by one year from SSN(m).

Comparing the minimums of SSA(N) and SSA(S), they occurred simultaneously in 7 of 13 SCs, including SC14, SC16 and SC19–SC23. Comparing the maximums of SSA(N) and SSA(S), they have occurred simultaneously in only 1 of 13 SCs (SC15). The maximum SSA(S) usually occurs after the maximum SSA(N), true for 9 of 13 SCs. For SC16, SC18, and SC19, the maximum SSA(S) occurred earlier than the maximum SSA(N). The mean SSA(N) measures 425.0 millionths of a solar hemisphere ($sd = 399.5$ millionths of a solar hemisphere), while the mean SSA(S) measures 412.5 millionths of a solar hemisphere ($sd = 381.4$ millionths of a solar hemisphere); hence, there is no statistically significant difference in the hemispheric means based on SSA.

Interesting is that many SCs have multiple peaks in SSA(N) and SSA(S), typically 2–3 years apart. Such behavior is clearly seen in SC12, SC13, SC16, SC18, SC19, and SC21 in SSA(N) and SC14, SC15, SC20, and SC22 in SSA(S). The rankings of maximum SSA(N) from least to greatest are as follows: SC12 (452.0); SC24 (561.4); SC13 (602.0); SC16 (725.9); SC14 (749.3); SC15 (853.6); SC23 (922.8); SC20 (1033.6); SC18 (1,180.2); SC21 (1,289.9); SC17 (1,316.1); SC22 (1,363.8); and SC19 (2,277.2). The rankings of maximum SSA(S) from least to greatest are as follows: SC14 (600.3); SC15 (680.4); SC16 (681.9); SC20 (683.3); SC12 (820.9); SC24 (940.8); SC13 (944.0); SC23 (1,103.9); SC17 (1,129.2); SC21 (1,227.1); SC22 (1,555.8); SC19 (1,608.8) and SC18 (1,642.9). On average, the maximum SSA(N) measures 1,025.2 millionths of a solar hemisphere ($sd = 482.1$) and the maximum SSA(S) measures 1,047.6 millionths of a solar hemisphere ($sd = 370.2$). The average time from minimum to maximum SSA(N) is 3.8 years (range 2–5 years), while the average time from minimum to maximum SSA(S) is 4.8 years (range 3–6 years). The average time from maximum to minimum SSA(N) is 6.9 years (range 5–9 years), while the average time from maximum to minimum SSA(S) is 6.2 years (range 5–8 years). For SC24, the elapsed time from its maximum to minimum SSA(N) for SC25 measures at least 6 years (if 2018 marks the occurrence of the minimum of SSA(N) for SC25), while the elapsed time from maximum to minimum SSA(S) for SC25 measures, at least 5 years (presuming 2019 marks the occurrence of minimum SSA(S) for SC25).

Figure 2 shows the yearly hemispheric variation of NARE, following the same format used in figure 1. Regarding figure 2a, it shows that the maximum in NARE(N) per SC increased between SC12 and SC19 and decreased between SC19 and SC24, as it occurred with SSA(N). SC19 had the largest yearly NARE(N), numbering 3,173 entries and occurring in 1959, some 2 years after SC19 SSN(M), as also was seen for SSA(N). The timing of the maximum for NARE(N) has occurred simultaneously with SSN(M) for only 6 of 13 SCs. For SC12, SC20, and SC24, the timing of maximum NARE(N) preceded SSN(M), while for SC18, SC19, and SC23, maximum NARE(N) followed SSN(M). Minimum NARE(N) nearly always has occurred simultaneously with SSN(m), with only SC12, 15, and 17 having minimum NARE(N) occurrences that differed by one year from SSN(m). Regarding figure 2b, it shows that the maximum in NARE(S) per SC also increased, especially, between SC14 and SC18–SC22 and decreased afterwards through SC24. The largest yearly NARE(S) numbered 2,917 entries and occurred in 1991 (SC22). The timing of the maximum of NARE(S) is found to have followed SSN(M) in 6 of 13 SCs, occurred simultaneously in 5 of 13 SCs and preceded by one year only in SC16 and 20. Like NARE(N), the minimum in NARE(S) usually occurs simultaneously with SSN(m), with only SC12, SC15, and SC17 having minimum NARE(S) occurrences that differed by one year from SSN(m).

Comparing the minimums of NARE(N) and NARE(S), they occurred simultaneously in 5 of 13 SCs, including SC14, SC16, SC19, SC22, and SC23. Comparing maximums of NARE(N) and NARE(S), they have occurred simultaneously in only 4 of 13 SCs, including SC13, SC15, SC20, and SC21. The maximum NARE(S) usually occurs after the maximum NARE(N), true for 7 of 13 SCs, including SC12, SC14, SC17, SC19, and SC22–SC24. For SC16 and SC18, the maximum NARE(S) occurred earlier than the maximum NARE(N). The mean NARE(N) measures 873.3 entries ($sd = 703.6$), while the mean NARE(S) measures 852.7 entries ($sd = 680.6$); hence, as with SSA, there is no statistically significant difference in the hemispheric means of NARE.

Double-peaking is found to have occurred in SC12, SC16, SC18, SC20 and SC21 for NARE(N) and in SC14, SC20, SC21 and SC23 for NARE(S), typically 2 years apart. The rankings of maximum NARE(N) from least to greatest are as follows: SC12 (895), SC24 (1,194), SC14 (1,235), SC13 (1,264), SC16 (1,301), SC23 (1,863), SC15 (1,938), SC17 (2,114), SC20 (2,159), SC18 (2,177), SC22 (2,532), SC21 (2,904) and SC19 (3,173). The rankings of maximum NARE(S) from least to greatest are as follows: SC14 (1,053), SC12 (1,206), SC24 (1,251), SC16 (1,428), SC15 (1,572), SC20 (1,622), SC17 (1,711), SC13 (1,808), SC23 (1,940), SC18 (2,368), SC21 (2,534), SC19 (2,560) and SC22 (2,917). On average, the maximum NARE(N) numbers 1,903.8 entries ($sd = 703.2$), while on average, the maximum NARE(S) numbers 1,843.8 entries ($sd = 586.2$). The average time from minimum to maximum NARE(N) is 4.0 years (range 3–5 years), while the average for NARE(S) is 4.6 years (range 3–6 years). For NARE(N), six SCs had intervals of rise (minimum to maximum) of 3 years, including SC12, SC17, SC20–SC22, and SC24, while six SCs had intervals of rise of 5 years, including SC14–SC16, SC18, SC19, and SC23. For NARE(S), four SCs had intervals of rise of 4 years, including SC15, SC16, SC18, and SC21, while, four SCs had intervals of rise of 5 years, including SC17, SC20, SC22, and SC24 and three SCs had intervals of rise of six years, including SC12, SC14, and SC23. (Obviously, strong linear correlations exist between SSN, SSA, and NARE.)

Figure 3 shows the yearly hemispheric variation of MAE. For both hemispheres, MAE appears to have multiple peaks. Also, there appears to be a downward trend in MAE for both hemispheres between SC12 and SC15, followed by an upward trend between SC15 and SC18/19 and another downward trend between SC18/19 and SC24, one that is more pronounced in the N hemisphere than in the S hemisphere. The means for the two hemispheres are not statistically different.

A comparison of the minimum MAE(N) with SSN(m) (see table 2) reveals that 7 of 13 SCs had simultaneous occurrences (i.e., no lag), 3 had minimum MAE(N) prior (1–2 years) to SSN(m), and 3 had minimum MAE(N) after (+1 year) SSN(m). A comparison of minimum MAE(S) with SSN(m) reveals that 8 of 13 SCs had simultaneous occurrences, 4 had minimum MAE(S) prior (1–2 years) to SSN(m), and 1 (SC24) had minimum MAE(S) after (+1 year) SSN(m). Minimum MAE(N) and MAE(S) for SC25 may have occurred, respectively, in 2018 and 2019. Hence, SSN(m) for SC25 should be expected sometime about 2016–2019 based on the minimum occurrence of MAE(N) and about 2017–2020 based on the minimum occurrence of MAE(S). In terms of SSN, it decreased in value between 2016 and 2019, measuring 39.9 in 2016, 7.0 in 2018, and 3.6 in 2019. Clearly, SSN(m) for SC25 is near, expected to occur either in 2019 or 2020. (SSN(m) for SC25 occurred in 2019.)

The rankings from least to greatest maximum MAE(N) are as follows: SC24 (187), SC22 (197), SC13 (199), SC15 (208), SC12 (213), SC16 (218), SC20 (222), SC23 (222), SC14 (239), SC21 (249), SC19 (262), SC17 (267), and SC19 (293). In terms of rankings from least to greatest

maximum MAE(S), it is as follows: SC20 (176), SC16 (199), SC22 (200), SC14 (208), SC15 (209), SC23 (212), SC24 (229), SC21 (231), SC13 (235), SC17 (241), SC19 (246), SC18 (253) and SC12 (265). The maximum MAE(N) tends to occur before the maximum MAE(S), true for 8 of 13 SCs. On average, the maximum MAE(N) measures 229 millionths of a solar hemisphere ($sd = 31$ millionths of a solar hemisphere), and the maximum MAE(S) measures 223 millionths of a solar hemisphere ($sd = 25$ millionths of a solar hemisphere).

Figure 4 depicts the yearly variations of the asymmetry based on NARE (top) and SSA (bottom). Asymmetric values near zero simply mean that both hemispheres are approximately of equal parametric magnitude, whereas asymmetric values of large magnitude indicate that one hemisphere is of greater parametric magnitude than the other hemisphere. The greatest positive or negative asymmetric values tend to occur near SSN(m). For Asymmetry (NARE), the maximum asymmetric value has occurred -3 to $+1$ years relative to SSN(m) occurrence. For Asymmetry (SSA), the maximum asymmetric value has occurred -3 to $+2$ years relative to SSN(m) occurrence. Large positive asymmetric values (the largest on record) occurred in 2019 for both NARE and SSA. Hence, one expects SSN(m) for SC25 to very probably occur very soon (i.e., sometime between 2019 and 2022, assuming the year 2019 marks the greatest asymmetric value year). For 11 of 13 SCs, maximum Asymmetry (SSA), ignoring sign, occurs either simultaneously with SSN(m) (SC12, SC13, SC17, and SC23) or before SSN(m) (SC14, SC15, SC18, SC19, SC21, SC22, and SC24).

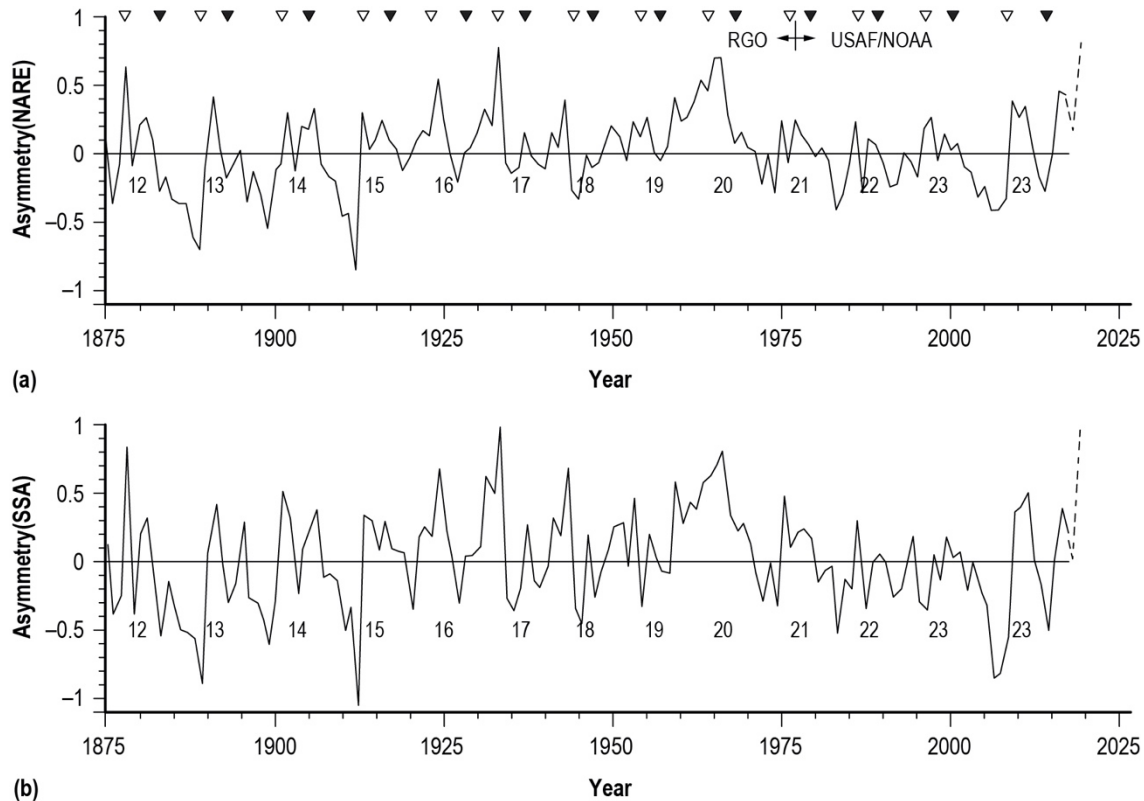


Figure 4. Annual variation of (a) Asymmetry(NARE) and (b) NARE(SSA).

Table 3 gives the parametric *m* and *M* values and the mean and *sd* values for SC12–SC24 and for even- and odd-numbered cycles (SC24 values are incomplete). Figure 5 depicts the *m* parametric cyclic variations (top) for SC12–SC25 and the *M* parametric variations (bottom) for SC1–SC24 (i.e., using the combined hemispheres). Figure 6 shows the *m* (top) and *M* (bottom) parametric cyclic hemispheric variations for SC12–SC25 and SC12–SC24, respectively. The downward pointing arrows in figures 5 and 6 denote that the true *m* values for SC25 could be smaller than shown, especially if SSN(*m*) for SC25 occurs in 2020 or later. The largest parametric *m* values occurred in SC21 (fig. 5), while the largest parametric *M* values occurred (fig. 5) in SC18 (MAE), SC19 (SSN and SSA) and SC21 (NARE). The largest *m* value based on N hemispheric values occurred (fig. 6) in SC21 (SSA and MAE) and SC20 (NARE), while the largest *m* value based on southern hemispheric values occurred in SC23 (SSA), SC21 (NARE) and SC18 (MAE). The largest *M* values based on northern hemispheric values (Figure 6) occurred in SC19 (SSA and NARE) and SC18 (MAE), while the largest *M* values based on southern hemispheric values occurred in SC18 (SSA), SC22 (NARE) and SC12 (MAE).

Table 3. Parametric *m* and *M* values.

Cycle	SSN		SSA		NARE		MAE		SSA(N)		SSA(S)		NARE(N)		NARE(S)		MAE(N)		MAE(S)		
	<i>m</i>	<i>M</i>	<i>m</i>	<i>M</i>	<i>m</i>	<i>M</i>	<i>m</i>	<i>M</i>	<i>m</i>	<i>M</i>	<i>m</i>	<i>M</i>	<i>m</i>	<i>M</i>	<i>n</i>	<i>M</i>	<i>n</i>	<i>M</i>	<i>n</i>	<i>M</i>	
12	5.7	106.1	22.2	1,148.9	81	2,039	100	234	11.9	452.0	1.7	820.9	53	895	15	1,206	82	213	41	265	
13	10.4	142.0	76.7	1,460.6	191	3,072	121	207	4.7	602.0	45.4	944.0	29	1,264	142	1,808	59	199	116	235	
14	4.6	105.5	27.9	1,195.9	78	1,951	100	225	21.2	749.3	6.6	600.3	36	1,235	42	1,053	82	239	57	208	
15	2.4	173.6	7.5	1,533.9	60	3,510	46	171	0.8	853.6	2.5	680.4	11	1,938	21	1,572	27	208	43	158	
16	9.7	129.7	54.7	1,388.9	244	2,613	82	209	32.6	725.9	22.0	681.9	138	1,301	106	1,428	86	218	76	199	
17	9.2	190.6	91.3	2,072.8	225	3,705	127	219	44.3	1,316.1	1.8	1,129.2	156	2,114	25	1,711	104	267	26	241	
18	16.1	214.7	124.7	2,634.1	370	4,298	123	235	42.2	1,180.2	45.9	1,642.9	135	2,177	152	2,368	114	293	110	253	
19	6.6	269.3	34.6	3,048.5	166	5,016	76	232	11.7	2,277.2	22.9	1,608.8	93	3,173	73	2,560	46	262	86	246	
20	15.0	150.0	53.9	1,601.3	390	3,390	51	194	44.1	1,033.6	9.8	683.3	284	2,159	77	1,622	57	222	34	176	
21	18.4	220.1	166.4	2,270.2	426	5,438	128	220	95.0	1,289.9	44.5	1,227.1	198	2,904	183	2,534	131	249	89	231	
22	14.8	211.1	123.2	2,572.0	394	4,751	108	198	80.4	1,363.8	42.8	1,555.8	242	2,532	152	2,917	104	197	103	200	
23	11.6	173.9	81.9	1,833.8	305	3,587	87	204	26.9	922.8	55.0	1,103.9	182	1,863	124	1,940	54	222	84	208	
24	4.2	113.3	22.9	1,251.0	122	2,442	69	187	5.0	561.4	7.9	940.8	41	1,194	38	1,548	45	172	76	229	
mean	9.9	169.2	68.3	1,847.1	235	3,524	94	210	32.4	1,025.2	23.8	1,047.6	123	1,904	88	1,867	76	228	72	219	
<i>sd</i>	5.1	50.6	48.0	619.3	132	1,116	28	20	29.0	482.1	20.2	370.2	88	703	58	567	31	33	30	31	
Even(7)																					
mean	10.0	147.2	61.4	1,684.6	240	3,069	90	212	33.9	866.6	14.1	989.4	133	1,642	83	1,735	81	222	71	219	
<i>sd</i>	5.3	47.5	44.8	645.1	146	1,107	25	20	25.2	334.7	15.4	431.7	99	631	55	669	24	38	29	32	
Odd(6)																					
mean	9.8	194.9	76.4	2,036.6	229	4,055	98	209	30.6	1,210.3	28.7	1,115.6	112	2,209	95	2,021	70	235	74	220	
<i>sd</i>	5.3	44.5	54.5	584.0	125	942	33	21	35.4	589.2	23.1	308.2	80	708	66	425	39	29	33	33	

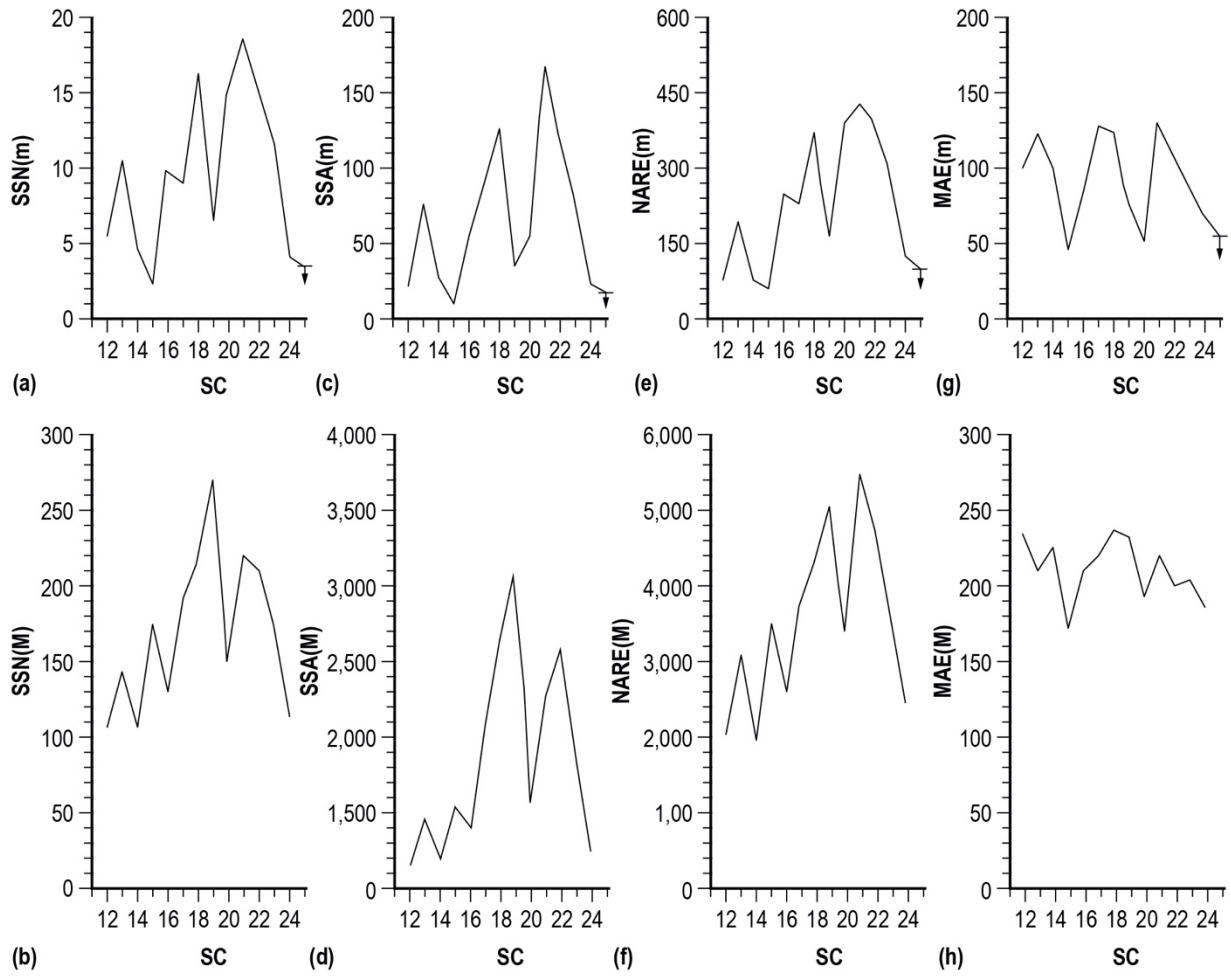


Figure 5. Cyclic variation of (a) SSN(m), (b) SSN(M), (c) SSA(m), (d) SSA(M), (e) NARE (m), (f) NARE(M), (g) MAE(m), and (h) MAE(M).

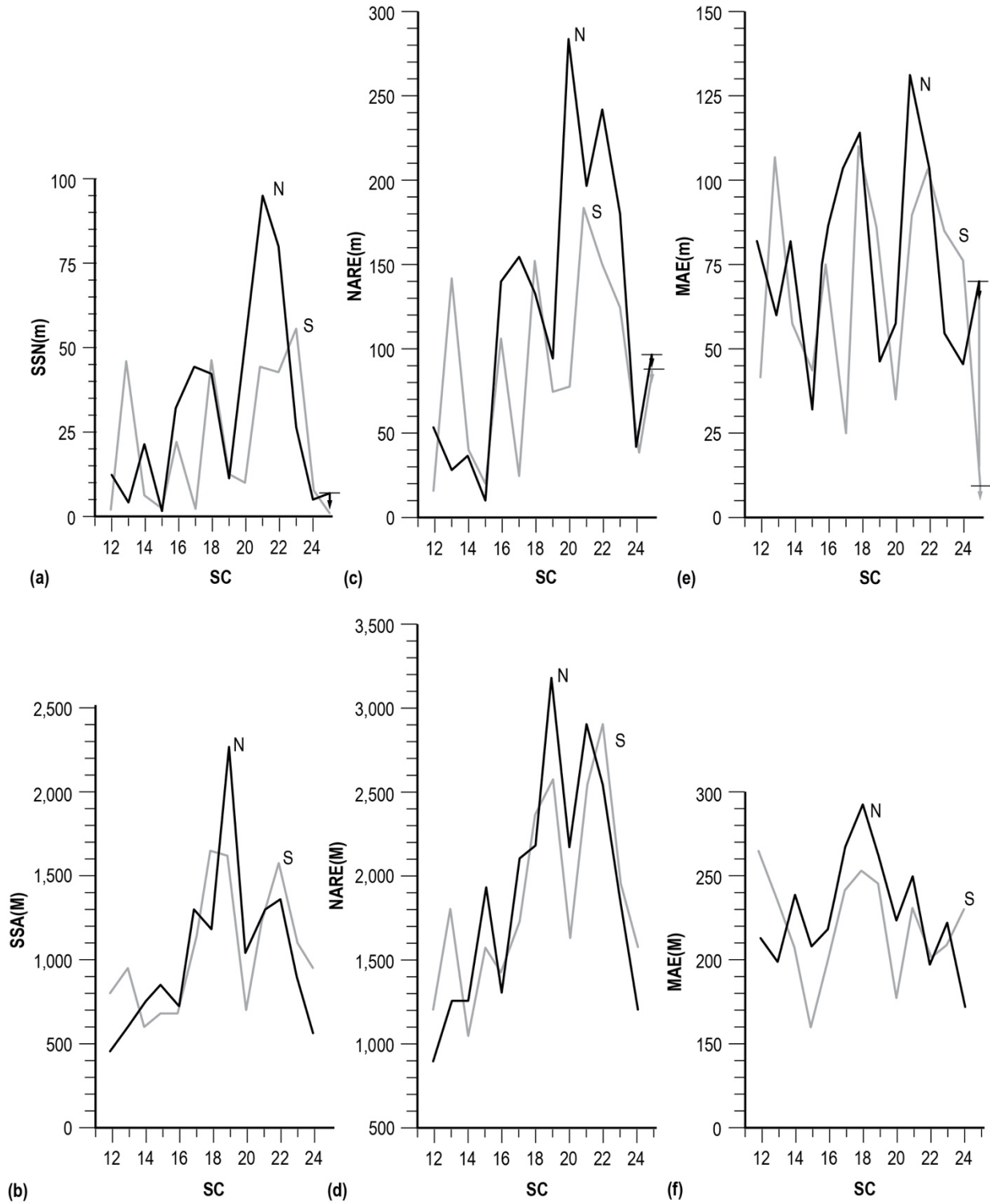


Figure 6. N-S cyclic variation of (a) SSA(m), (b) SSA(M), (c) NARE(m), (d) NARE(M), (e) MAE(m), and (f) MAE(M).

Figure 7 displays the parametric variations based on SC12–SC23 relative to SSN(m) for (a) SSA, (b) NARE, and (c) MAE. In the figure, the thicker darker line represents the northern hemispheric parametric mean; the thinner lighter line represents the southern parametric mean; the darker dotted line (filled circles) represents SC24 northern hemispheric values; and the lighter dotted line (unfilled circles) represents SC24 southern hemispheric values. Marked across the top are the SSN(M) occurrences for SC12–SC24. The $t = 10$ values for SC24 correspond to the yearly 2018 values (see table 1; the yearly 2019 values are lower still for SSN, SSA, SSA(S), MAE(S), NARE, NARE(N) and NARE(S)). Interesting is the behavior of SSA(N), NARE(N), and MAE(N) near SSN(m) for SC24. Comparison of the 2018 yearly values to values in 2006–2008 are suggestive that SC25(m) should be expected to occur within two years following 2018 (i.e., 2019 or 2020).

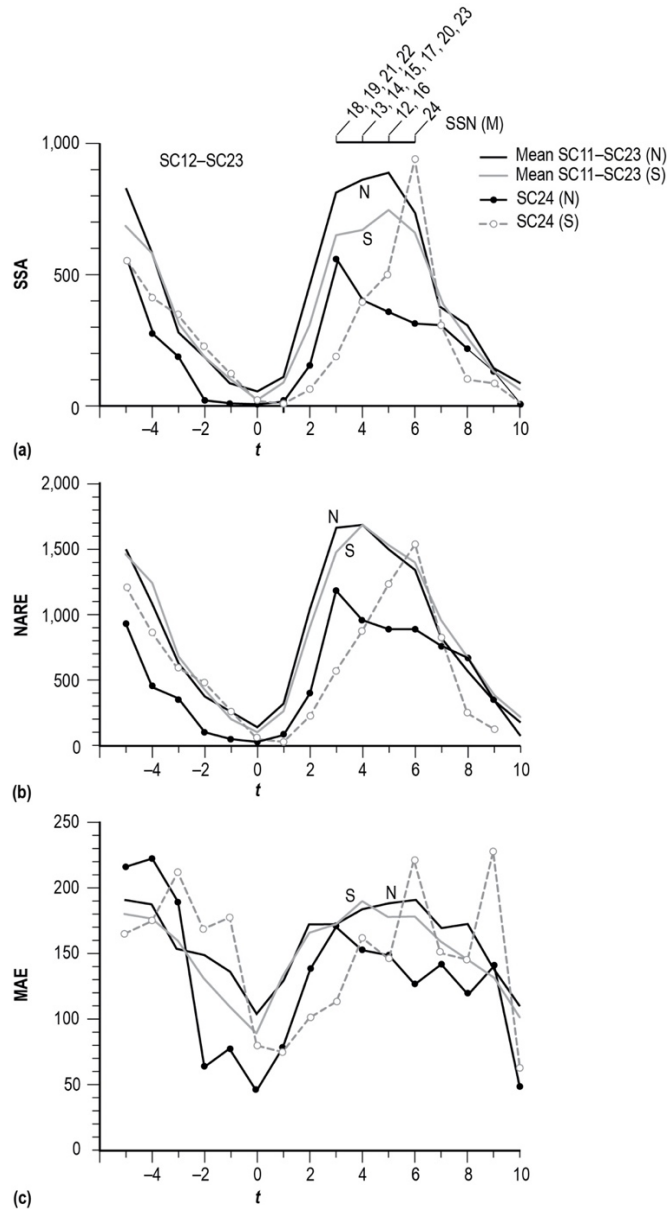


Figure 7. N-S variation of mean SC12–SC23 and annual SC24 values relative to SSN(m) for (a) SSA, (b) NARE and (c) MAE, for elapsed time t (in years) equal to -5 to $+10$.

Figure 8 is similar to figure 7 but now is plotted in terms of even- and odd-numbered SCs. For the odd-numbered SC, the plotted SC24 values presume SSN(m) for SC25 in 2019. If it turns out that the year 2020 marks the true occurrence of SSN(m) for SC25, then the plotted points must be shifted one year earlier (i.e., to the left). (SSN(m) for SC25 occurred in 2019.)

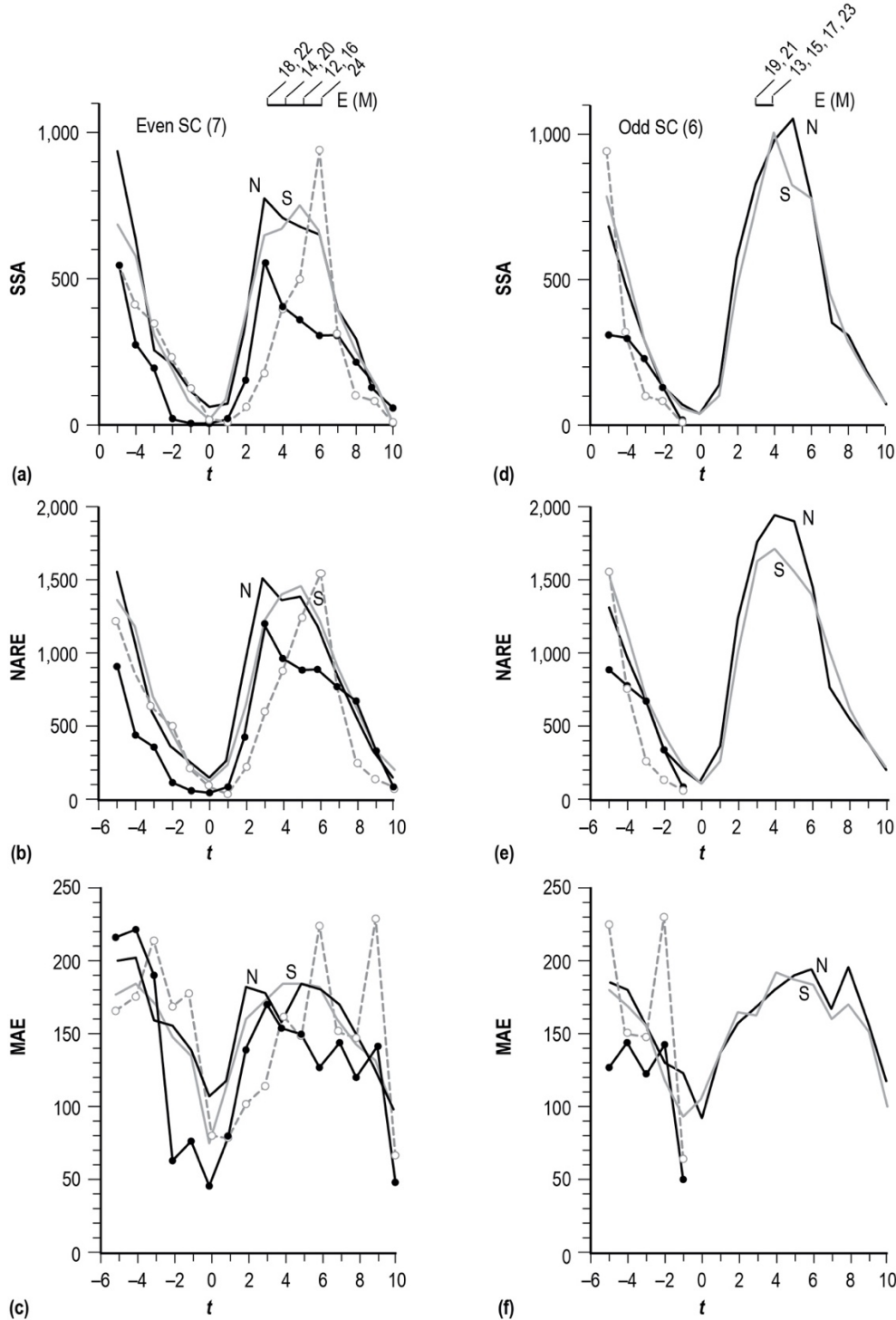


Figure 8. N-S variation of mean even- and odd-numbered SC and annual SC24 values relative to SSN(m) for (a) SSA, (b) NARE and (c) MAE, for elapsed time t (in years) equal to -5 to $+10$.

Figure 9 plots Asymmetry(SSA) and Asymmetry(NARE). Again, SC24 values are plotted assuming SSN(m) for SC25 occurred in 2019. The greatest negative Asymmetry(SSA) for SC24 occurred at $t = -2$ (2006), while the greatest positive Asymmetry(SSA) for SC24 appears to have occurred at $t = 11$ (2019, not shown; see table 1), surpassing the value at $t = +3$ (2011).

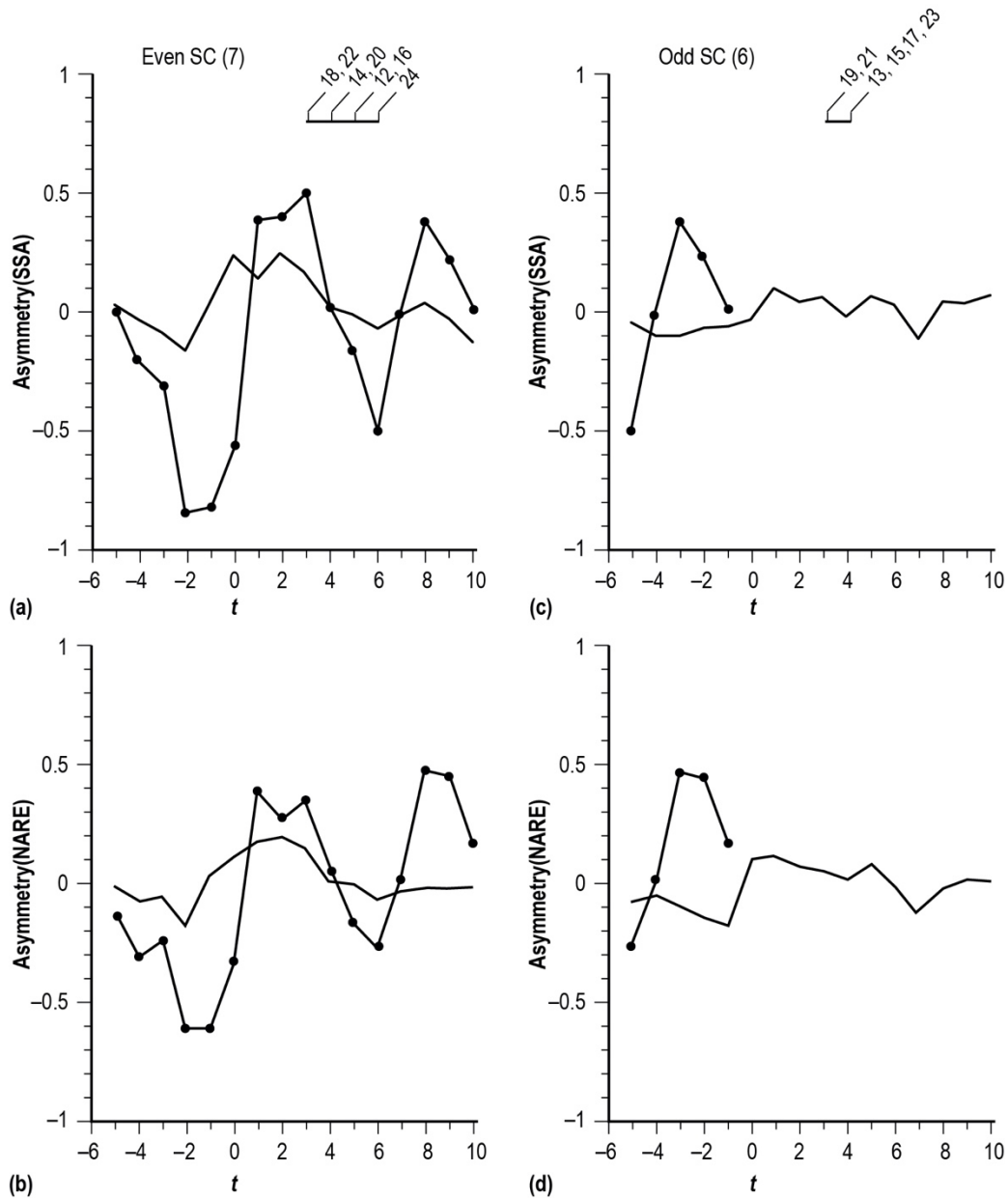


Figure 9. Variation of Asymmetry of mean of even- and odd-numbered SC and annual SC24 values relative to SSN(m) for (a) SSA and (b) NARE, for elapsed time t (in years) equal to -5 to $+10$.

Figure 10 simply shows the cyclic variation of LAAR/H. The northern hemisphere had the largest spots at minimum (m) in SC12, SC14–SC17, and SC21 and the largest spots at maximum (M) in SC12, SC16, SC17 and SC19–SC22. For SC24 the S hemisphere had the largest LAAR/H at both m and M. The largest LAAR/H at maximum occurred in SC18 in 1947 (SC18), measuring 6,132 millionths of a solar hemisphere, while the LAAR/H at minimum occurred in 1934 (SC17), measuring 1,169 millionths of a solar hemisphere.

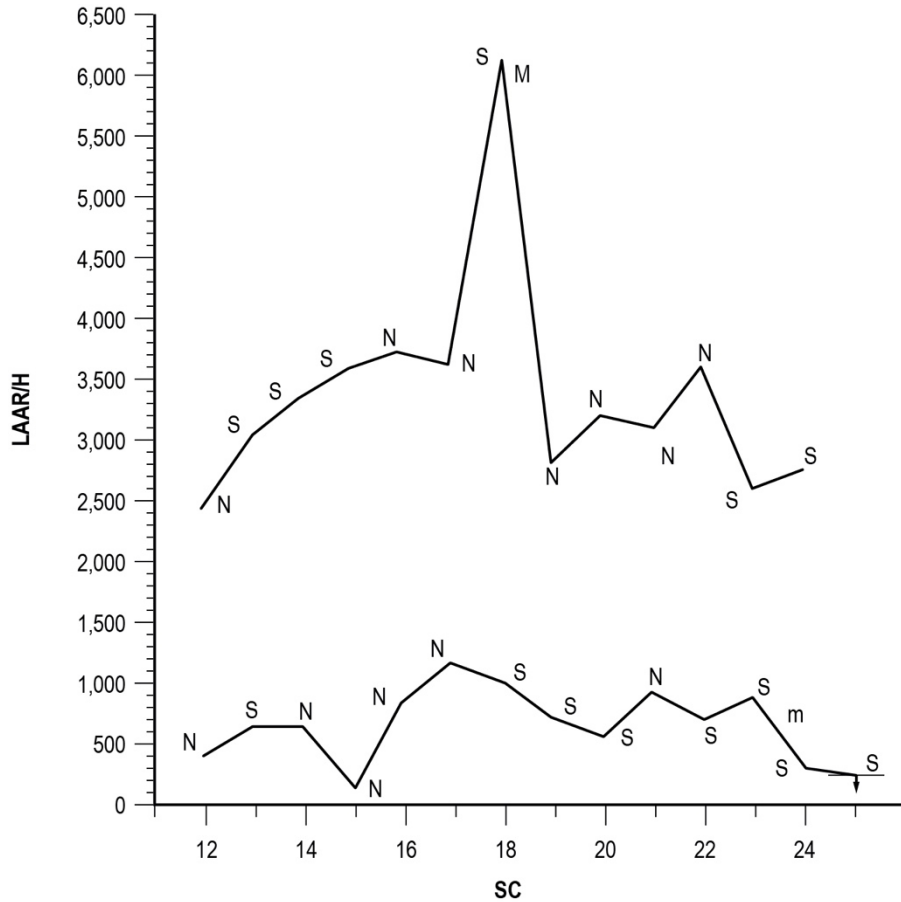


Figure 10. Cyclic variation of minimum and maximum LAAR/H.

Table 4 summarizes the behavioral dominance (i.e., number of years) of the N-S SSA per SC, both in terms of the overall SC and the ASC and DES intervals. For SC12–SC24, SSA(N) was larger than SSA(S), 75 versus 66 years. During the ASC interval, SSA(N) likewise, has been the more dominant, 35 versus 17 years, while during the DES interval, SSA(S) has been the more dominant, 49 versus 40 years. For even-numbered SCs, SSA(N) has been the more dominant overall and during the ASC interval, 43 versus 33 years, and 21 versus 9 years, respectively, while for odd-numbered SCs, SSA(S) has been the more dominant during the DES interval, 25 versus 18 years, while being less dominant during the ASC interval, 8 versus 14 years.

Table 4. N-S SSA dominance per SC.

Cycle	Overall		ASC		DES	
	N	S	N	S	N	S
12	3	8	3	2	0	6
13	3	9	2	2	1	7
14	5	7	3	1	2	6
15	9	1	4	0	5	1
16	9	1	4	1	5	0
17	5	6	1	3	4	3
18	5	5	1	2	4	3
19	7	3	2	1	5	2
20	8	4	4	0	4	4
21	4	6	3	0	1	6
22	6	4	2	1	4	3
23	4	8	2	2	2	6
24#	≥7	≥4	4	2	≥3	≥2
Total#	≥75	≥66	35	17	≥40	≥49
Even#	≥43	≥33	21	9	≥22	≥24
odd	32	33	14	8	18	25

Note: # means SC24 DES is unknown; excludes values for 2019.

In conclusion, this study has examined the N-S yearly variations of SSA, NARE, and MAE. For the overall interval of 1875–2019, the northern hemisphere has been the more dominant hemisphere in 77 of 145 years based on SSA. Likewise, for SC12–SC24, SSA(N) has been greater than SSA(S) during the ascending phase of the solar cycle (i.e., 35 of 52 years), whether the SC is an even- or odd-numbered SC, while SSA(S) has been greater than SSA(N) during the descending phase of the solar cycle (51 of 93 years). Minimum SSA(N) and SSA(S) have occurred in the same year in only 7 of 13 SCs including SC14, SC16, and SC19–SC23. Maximum SSA(N) and SSA(S) have occurred in the same year only once (in SC15). Maximum SSA(S) usually occurs after maximum SSA(N), true for 9 of 13 SCs. Maximum SSA(S) preceded maximum SSA(N) in SC16, SC18 and SC19. Multiple peaks in SSA(N) or SSA(S), typically 2–3 years apart, have often been seen (e.g., SC12–SC16 and SC18–SC22). SC12 had the smallest maximum SSA(N) (452.0 millionths of a solar hemisphere), while SC19 had the largest maximum SSA(N) (2,277.2 millionths of a solar hemisphere). SC14 had the smallest SSA(S) (600.3 millionths of a solar hemisphere), while SC18 had the largest SSA(S) (1,642.9 millionths of a solar hemisphere). The average time from minimum to maximum SSA(N) is 3.8 years (range 2–5 years), while it is 4.8 years for SSA(S) (range 3–6 years). The average time from maximum SSA(N) to the following minimum SSA(N) is 6.9 years (range 5–9 years), while it is 6.2 years for SSA(S) (range 5–8 years). The largest N-S asymmetry coefficients for SSA occurs between –3 and +1 year about sunspot minimum. The largest N-S asymmetry coefficient in SSA occurred in 2019 (SC24). The largest area sunspot occurred in 1947 (SC18), occurring in the southern hemisphere and measuring 6,132 millionths of a solar hemisphere, nearly twice the size of the average maxima of the largest area spots in the other 12 SCs. SSA and NARE are highly correlated with each other and with SSN. Minimum MAE(N) and MAE(S) may have occurred, respectively, in 2018 and 2019, highly suggestive that SSN(m) for SC25 either occurred in 2019 or will occur in 2020. (SSN(m) for SC25 is now known to have occurred in 2019.)

LITERATURE CITED

- Antalová, A. and M. N. Gnevyshev 1983. Latitudinal Distribution of Sunspot Areas during the Period 1874–1976, *Contributions of the Astronomical Observatory Skalnaté Pleso*, 11, pp. 63–93.
- Ataç, T. and A. Özgüç 1996. North-South Asymmetry in the Solar Flare Index, *Solar Physics*, 166, pp. 201–208.
- Badalyan, O. G. and V. N. Obridko 2011. North-South Asymmetry of the Sunspot Indices and Its Quasi-Biennial Oscillations, *New Astronomy*, 16(6), pp. 357–365.
- Ballester, J. L., R. Oliver, and M. Carbonell 2005. The Periodic Behaviour of the North-South Asymmetry of Sunspot Areas Revisited, *Astronomy and Astrophysics*, 431, pp. L5–L8.
- Carbonell, M., R. Oliver and J. L. Ballester 1993. On the Asymmetry of Solar Activity, *Astronomy and Astrophysics*, 274, pp. 497–504.
- Chang, H.-Y. 2007. Variation in North-South Asymmetry of Sun Spot Area, *Journal of Astronomy and Space Science*, 24(2), pp. 091–098.
- Chang, H.-Y. 2008. Stochastic Properties in North-South Asymmetry of Sunspot Area, *New Astronomy*, 13(4), pp. 195–201.
- Chowdhury, P., D. P. Choudhary, and S. Gosain 2013. A Study of the Hemispheric Asymmetry of Sunspot Area during Solar Cycles 23 and 24, *The Astrophysical Journal*, 768(2), pp. 188–198.
- Donner, R. and M. Thiel 2007. Scale-Resolved Phase Coherence Analysis of Hemispheric Sunspot Activity: A New Look at the North-South Asymmetry, *Astronomy and Astrophysics*, 475(3), pp. L33–L36.
- Duchlev, P. I. and V. N. Dermendjiev 1996. Periodicities in the N-S Asymmetry of Long-Lived Solar Filaments, *Solar Physics*, 168, pp. 205–210.
- Garcia, H. A. 1990. Evidence for Solar-Cycle Evolution of North-South Flare Asymmetry during Cycles 20 and 21, *Solar Physics*, 127, pp. 185–197.
- Joshi, B. and A. Joshi 2004. The North-South Asymmetry of Soft X-Ray Flare Index during Solar Cycles 21, 22 and 23, *Solar Physics*, 219, pp. 343–356.
- Kiepenheuer, K. O. 1953. Chapter 6. Solar Activity, *The Sun*, G. P. Kuiper (ed.), *The Solar System*, Vol. I, The Univ. Chicago Press, Chicago, IL, pp. 322–465.
- Knaack, R., J. O. Stenflo, and S. V. Berdyugina 2004. Periodic Oscillations in the North-South Asymmetry of the Solar Magnetic Field, *Astronomy and Astrophysics*, 418, pp. L17–L20.
- Li, K. J. 2009. Systematic Time Delay of Hemispheric Solar Activity, *Solar Physics*, 255, pp. 169–177.
- Li, K. J., J. X. Wang, S. Y. Xiong, H. F. Liang, H. S. Yun and X. M. Gu 2002. Regularity of the North-South Asymmetry of Solar Activity, *Astronomy and Astrophysics*, 383, pp. 648–652.
- Li, K. J., H. D. Chen, L. S. Zhan, Q. X. Li, P. X. Gao, J. Mu, X. J. Shi and W. W. Zhu 2009. Asymmetry of Solar Activity in Cycle 23, *Journal of Geophysical Research*, 114, 6 pp.
- Li, K. J., P. X. Gao and L. S. Zhan 2008. The Long-Term Behavior of the North-South Asymmetry of Sunspot Activity, *Solar Physics*, 254(1), pp. 145–154.

- Li, K. J., P. X. Gao, L. S. Zhan and X. J. Shi 2009. The Long-Term Hemispheric Sunspot Activity, *The Astrophysical Journal*, 691(1), pp. 75–82.
- Maunder, E. W. 1922. The Sun and Sunspots, 1820-1920, *Monthly Notices of the Royal Astronomical Society*, 82, pp. 534–543.
- Newcomb, S. 1901. On the Period of the Solar Spots, *The Astrophysical Journal*, 13(1), pp. 1–14.
- Newton, H. W. and A. S. Milson 1955. Note on the Observed Differences in Spottedness of the Sun's Northern and Southern Hemispheres, *Monthly Notices of the Royal Astronomical Society*, 115, pp. 398–404.
- Oliver, R. and J. L. Ballester 1994. The North-South Asymmetry of Sunspot Areas during Solar Cycle 22, *Solar Physics*, 152, pp. 481–485.
- Roy, J.-R. 1977. The North-South Distribution of Major Solar Flare Events, Sunspot Magnetic Classes and Sunspot Areas (1955–1974), *Solar Physics*, 52, pp. 53–61.
- Schlamming, L. 1991. Hemispherical Asymmetries in Sunspot Areas and Auroral Frequencies, *Solar Physics*, 135, pp. 407–413.
- Swinson, D. B., H. Koyama, and T. Saito 1986. Long-Term Variations in North-South Asymmetry of Solar Activity, *Solar Physics*, 106, pp. 35–42.
- Temmer, M., A. Veronig, and A. Hanslmeier 2002. Hemispheric Sunspot Numbers R_n and R_s : Catalogue and N-S Asymmetry Analysis, *Astronomy and Astrophysics*, 390, pp. 707–715.
- Temmer, M., J. Rybak, P. Bendik, A. Veronig, F. Vogler, W. Otruba, W. Potzi, and A. Hanslmeier 2006. Hemispheric Sunspot Numbers R_n and R_s from 1945-2004: Catalogue and N-S Asymmetry Analysis for Solar Cycles 18-23, *Astronomy and Astrophysics*, 447(2), pp. 735–743.
- Vernova, E. S., K. Mursula, M. I. Tyasto, and D. G. Baranov 2002. A New Pattern for the North South Asymmetry of Sunspots, *Solar Physics*, 205, pp. 371–382.
- Vernova, E. S., K. Mursula, M. I. Tyasto, and D. G. Baranov 2004. Long-Term Longitudinal Asymmetries in Sunspot Activity: Difference between the Ascending and Descending Phase of the Solar Cycle, *Solar Physics*, 221, pp. 151–165.
- Vizoso, G. and J. L. Ballester 1987. North-South Asymmetry in Sudden Disappearances of Solar Prominences, *Solar Physics*, 112, pp. 317–323.
- Vizoso, G. and J. L. Ballester 1990. The North-South Asymmetry of Sunspot, *Astronomy and Astrophysics*, 229, pp. 540–546.
- Waldmeier, M. 1971. The Asymmetry of Solar Activity in the Years 1959-1969, *Solar Physics*, 20, pp. 332–344.
- Watari, S. 1996. Chaotic Behavior of the North-South Asymmetry of Sunspots? *Solar Physics*, 163, pp. 259–266.
- Wilson R. M. 2019a. Predicting the Size and Timing of the Next Solar Cycle: Paper I, based on Sunspot Number, *Journal of the Alabama Academy of Science*, 90(2), pp. 70–92.
- Wilson R. M. 2019b. Predicting the Size and Timing of the Next Solar Cycle: Paper II, based on Geomagnetic Values, *Journal of the Alabama Academy of Science*, 90(2), pp. 93–109.

- Wilson, R. M. 2020. An Examination of the Sunspot Areal Dataset, 1875–2017: Paper I, an Overview, *Journal of the Alabama Academy of Science*, in press.
- Yi, W. 1992. The North-South Asymmetry of Sunspot Distribution, *Journal of the Royal Astronomical Society of Canada*, 86, pp. 89–98.
- Zharkov, S., V. V. Zharkova and S. S. Ipson 2005. Statistical Properties of Sunspots in 1996-2004:
I. Detection, North-South Asymmetry and Area Distribution, *Solar Physics*, 228, pp. 377–397.
- Zolotova, N. V. and D. I. Ponyavin 2006. Phase Asynchrony of the North-South Sunspot Activity, *Astronomy and Astrophysics*, 449, pp. L1–L4.
- Zolotova, N. V. and D. I. Ponyavin 2007. Synchronization in Sunspot Indices in the Two Hemispheres, *Solar Physics*, 243, pp. 193–203.
- Zolotova, N. V., D. I. Ponyavin, N. Marwan, and J. Kurths 2009. Long-Term Asymmetry in the Wings of the Butterfly Diagram, *Astronomy and Astrophysics*, 503, pp. 197–201.